China Geology 7 (2024) 653−660

China Geology

Journal homepage: http://chinageology.cgs.cn
https://www.sciencedirect.com/journal/china-geology

Pacific oyster (*Crassostrea gigas*) shell growth duration in a year in Bohai Bay and implication for its carbon sink potential

Wen-yu Wang[a], Chang-fu Fan[b,*], Zhao-jun Song[c], Hong Wang[d], Fu Wang[d]

[a] *Qingdao Geotechnical Investigation and Surveying Research Institute*, *Qingdao* 266033, *China*
[b] *MRL Key laboratory of Metallogeny and Mineral Assessment*, *Institute of Mineral Resources*, *Chinese Academy of Geological Sciences*, *Beijing* 100037, *China*
[c] *College of Earth Science and Engineering*, *Shandong University of Science and Technology*, *Qingdao* 266590, *China*
[d] *Tianjin Centre*, *China Geological Survey*, *Tianjin* 300170, *China*

ARTICLE INFO

Article history:
Received 16 November 2022
Received in revised form 26 August 2023
Accepted 1 September 2023
Available online 8 September 2023

Keywords:
Crassostrea gigas
Winter freeze shock
Oxygen isotope
Bohai Bay
Carbon sequestration and storage
Environmental geological survey

ABSTRACT

Oyster is a bivalve mollusk widely distributed in estuarine and shallow sea environments. Its growth and burial process is a carbon sequestration and storage process. Oyster shell may stop growing due to suffer from freeze shock during the winter season within a temperate climate, therefore, in order to study the carbon sequestration capacity of oysters we need to know the water temperature at which the shell suffer from winter freeze shock. This study examines $\delta^{18}O$ profiles across consecutive micro-growth layers found in three modern Pacific oyster shells from the northwest coast of Bohai Bay. A total of 165 oxygen isotope values from sequential samples of their left shells showed periodically varying values, and the variation fluctuation of oxygen isotope values was 4.97‰ on average. According to the variation range of the oxygen isotope value of the shell, combined with the sea surface temperature and the sea surface salinity data of the water in which the oysters grew, the water temperature that suffer from winter freeze shock and stops or retards the growth of Pacific oysters in Bohai Bay is about 8.3°C, and the corresponding period is from December to March of the following year. The calcification time of oysters within one year is nearly a month longer than previously thought, therefore, its carbon sink potential is also improved.

1. Introduction

The Pacific oyster (*Crassostrea gigas*) is characterized by high tolerance of variations in water temperature, a high rate of reproduction, and a high rate of colonization in a wide range of Pacific coastal waters (Cognie B et al., 2006; Diederich S 2005). *C. gigas* prefers a firm substrate and usually attaches to rocks, debris, or other oyster shells; it is also found on mud or mud-sand bottoms. Therefore, reefs composed of oyster shells are widely distributed in various types of estuarine and coastal areas from low latitudes to mid-high latitudes. At present, many researches mainly focus on the water purification function (Quan WM et al., 2006; Jackson JB et al., 2001; Quan WM et al., 2007; Gao LJ et al., 2006) and ecological function (Peterson CH et al., 2003; Dame RF 1987) of oyster reef. There are few studies on oyster reefs with strong carbon sequestration and carbon storage functions, which can effectively reduce seawater CO_2 concentration (Peterson CH et al., 2003; Dame RF et al., 1989). Like salt marshes, seagrasses, and mangroves, shellfish reef ecosystems contribute to localized mass burial of newly fixed, excess, organic carbon, and thus may play a notable role in mitigating atmospheric build-up of CO_2. In addition, oyster reefs can also indirectly contribute to the carbon neutralization process by protecting other blue carbon ecosystems such as salt marshes and seagrass beds from storm and flood damage (Fodrie FJ et al., 2017).

When the oyster larvae are fixed, they can continuously use HCO_3^- and Ca^{2+} in the water to form calcium carbonate ($CaCO_3$) shell, This process is called calcification, and the chemical reaction is: $Ca^{2+}+2HCO_3^-=CaCO_3+CO_2+H_2O$. The carbon sequestration capacity of oysters is mainly through the calcification of oyster shells (Shen XQ et al., 2011). The inorganic carbon (calcium carbonate) stored in the oyster shell

First author: *E-mail address*: 919995771@qq.com (Wen-yu Wang).

* Corresponding author: *E-mail address*: tjfchangfu@163.com (Chang-fu Fan).

Literary editor: Li-qiong Jia
doi:10.31035/cg2023054
2096-5192/© 2024 China Geology Editorial Office.

through the calcification process can exist in the natural state for thousands of years (Shen XQ et al., 2011; Li J et al., 2016; Zhang YY et al., 2017). In the process of calcification, oysters absorb bicarbonate to form calcium carbonate shells and release CO_2 to the atmosphere (Arrhenius S, 1896; Taylor AH et al., 1991), and the acidity of water will also increase (Broecker WS et al., 1966). Whether this process is the sink or source of atmospheric CO_2 is controversial. Therefore, to study the carbon sequestration process and carbon sink potential of oyster shells, it is necessary to fully understand the growth information of the shell.

At present, more than 50 buried oyster reefs and modern living oyster reefs have been found on the west coast of Bohai Bay (Li JF et al., 2020). Oyster reefs are mainly composed of *C.gigas*. Oyster shells are biological calcium carbonate ($CaCO_3$) and crystal forms are authigenic calcite (Wang H et al., 1995). Fan CF et al. (2011) demonstrated that Pacific oyster (*C. gigas*) preserves a sclerochronological record on the cross sections of the left valve in the form of gray translucent and white opaque band. The gray translucent band was formed during winter freeze shock and spawning in spring season, the white opaque band was formed during the normal growth of the shell, these three growth bands correspond to different forms of resilifer surface. The gray translucent growth bands in the cross section corresponding to the concave bottoms on resilifer surface of the shell had the heaviest $\delta^{18}O$ in an annual growth cycle, which were formed during lowest temperature recorded by shell in winter seasons (Fan CF et al., 2011). Oyster shell growth may suffer from winter freeze shock within a temperate climate (Wang H et al., 1995; Wang H et al., 2006; Fan CF et al., 2011; Ullmann C et al., 2010). Therefore, when study the carbon sink potential of Pacific oysters, it needed to know the water temperature experienced by the Pacific oyster in winter while it encounters winter freeze shocks, which is an important factor in determining how long the shells can grow in a year.

In this study, the authors examined the oxygen isotopes of three modern oyster shells collected from the northwest coast of Bohai Bay in order to investigate the mean inter-annual variation range of oxygen isotopes, combined with the sea surface temperature and the sea surface salinity data of the water in which the oysters grew, to determine the lowest water temperature recorded in winter by the Pacific oyster in the Bohai Bay while it encounters the winter freeze shock. Accurate freeze shock temperature and time can provide necessary basic information for studying the growth time and evaluating the carbon sink potential of oyster shells, and also provides quantitative data support for guiding reef building and initiative to construct the "China Coastal Oyster Reef Eco-Corridor" (Yang D et al., 2022).

2. Regional setting

The Bohai Sea is a shallow, semi-enclosed marginal sea in the western Pacific Ocean, located at the northwestern end of the Yellow Sea (Fig. 1). It has three major bays, with its east-

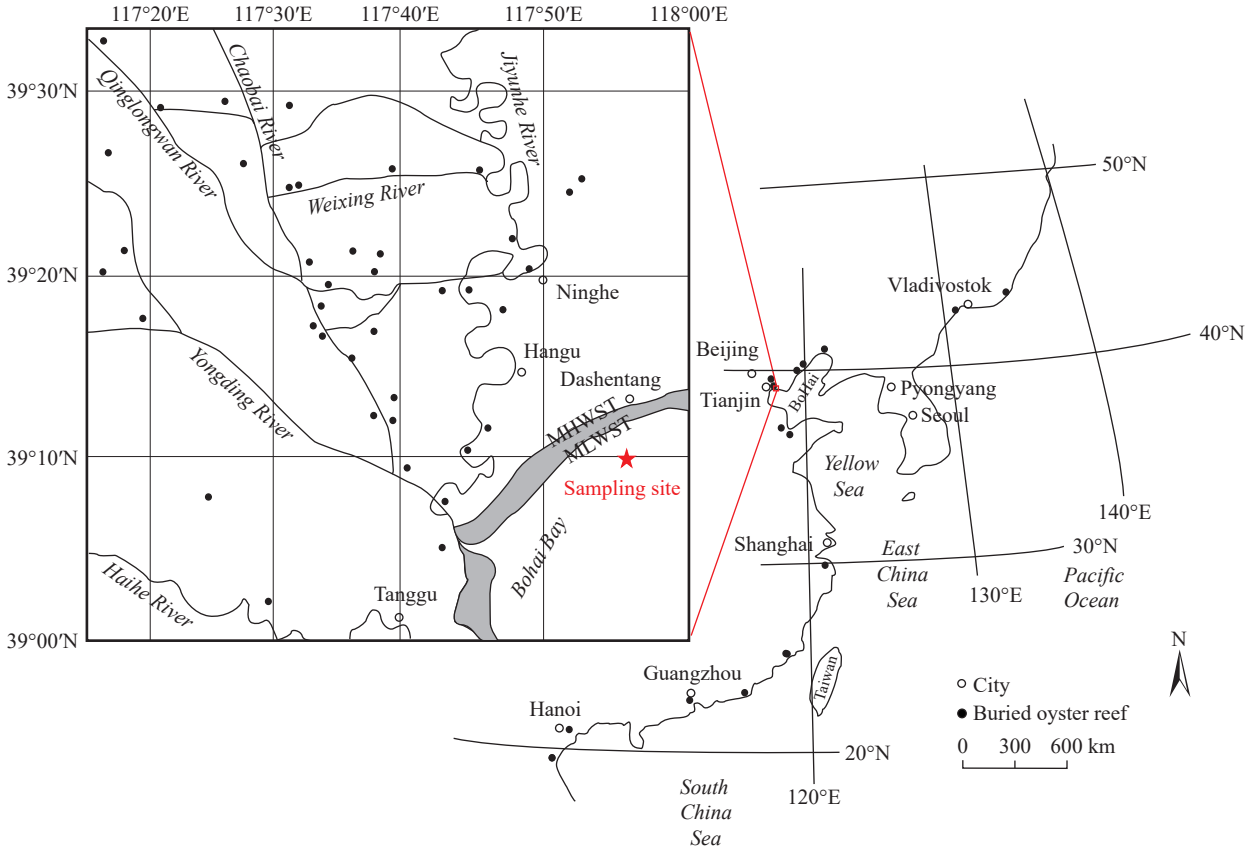

Fig. 1. Map showing the distribution of buried and living oyster reefs on the northwest coast of Bohai Bay and the sampling site for this study (modified from Wang H et al., 2006).

west width approximately 300 km and north-south length approximately 550 km and an area of approximately 77000 km^2. The Bohai Sea is subjected to the East Asian monsoon, meaning wind directions from the north to southwest prevail in winter, whereas in summer the winds are mainly from the south. The hydrology of the Bohai Sea is also influenced by variations in climate (Hainbucher D et al., 2004) that a rising trend has been documented for both sea surface temperature (SST) and sea surface salinity (SSS). The SST increase appears to be correlated with variations in air temperature, with the SST changes lagging behind changes in air temperature (Zou HC, 1988). The present level of SSS is approximately 2.5‰ higher than that 40 years ago (Hainbucher D et al., 2004).The evolution of salinity is determined by evaporation, precipitation, and river runoff in coastal area (Fan CF et al., 2011).

The present-day shallow sea of Bohai Bay contains a living, natural oyster reef (Fig. 1) that consists of *C. gigas*. The reef has been badly damaged by fishing and is divided into three sub-reefs. Side scan sonar mapping indicates that the reef has a total area of approximately 3 km^2. The living shells within the reef are much smaller than the buried shells in the coastal plain, most of the living shells are less than 10 cm length and are less than 4 years old (Fan CF et al., 2011).

SST, and precipitation at the living oyster reef show clear seasonality, SSS is negatively correlated with precipitation (Fig. 2). During the period 2005–2009, average monthly seawater temperatures varied typically between −0.7°C and 27.1°C between winter and summer, the highest SST recorded was 27.5°C, and average monthly salinity variations were low and differed by a maximum of 2.2‰ (Fan CF et al., 2011; Table 1). The salinity of these waters was high compared with that typically observed for oysters, reflecting a shortage of freshwater input from nearby rivers due to dam construction and the extraction of river water for irrigation in hinterland areas (Fan CF et al., 2011).

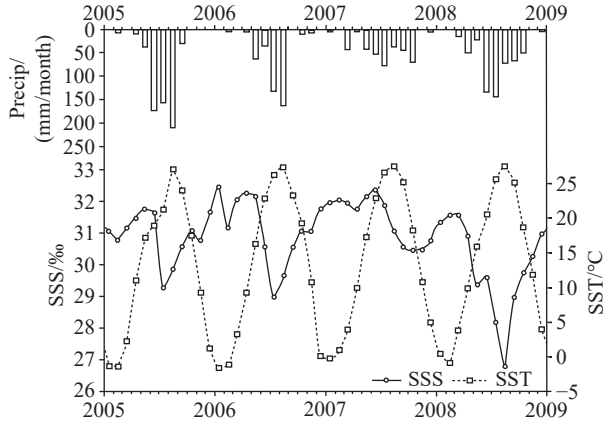

Fig. 2. Time series of salinity, temperature, and precipitation for the years 2005-2009 (Fan CF et al., 2011). Temperature and salinity measurements were taken near the modern living oyster reef by the State Ocean Information Center of China. Monthly averages were calculated from hourly measurements. Precipitation data were sourced from the Tianjin Statistical Yearbook.

The sampled living oyster reef is part of a shallow subtidal environment with water depths of 20 cm to 50 cm below the lowest tide level. This setting guarantees that the sampled specimens were continuously submerged in seawater, except under rare extreme conditions. Subaerial exposure may have occurred only during strong offshore winds combined with low tides.

3. Materials and methods

Three modern living specimens of *C. gigas* were collected on 26 May, 2005 from the living oyster reef. Immediately upon collection, the oyster was carefully opened in the field by cutting through the adductor muscle, avoiding damage to the hinge area. The flesh was scraped from the inner surface of the shell valves. Upon returning to the laboratory, the shell was washed in hydrogen peroxide and rinsed in demineralized water.

Three of the shells selected (ST2, ST25 and ST31) were sectioned from the ligament to the longest growth edge along a straight line, using a water-cooled diamond saw. The obtained cross-sections of the shell showed a layer of dense, foliated calcite under the resilifer. The cross-sections were polished using wettable carborundum discs (400–1200 grid) and then ultrasonically rinsed with demineralized water prior to the extraction of carbonate samples (Fan CF et al., 2011).

The growth Increments of *C. gigas* are large and easy to drill, and it is possible to obtain sufficient material while avoiding surficial contamination. High-resolution sampling was applied to all three shells and was accomplished using micro-Mill automatic micro-layer sampling system with a 0.3 mm stainless steel “V shape” drill needle (samples taken at 0.3 mm intervals) following the micro-growth increment patterns of translucent growth bands observed in cross-section. We also used the small cleft at the boundary between the resilifer surface and the inner shell layer, which corresponds to a translucent growth band viewed in cross-section, as an extra guideline for micro-sampling (Fan CF et al., 2011). Approximately 0.5 mg of carbonate powder was collected from each sample.

A total of 165 high-resolution samples from ST2, ST25, and ST31 were collected for δ^{18}O and δ^{13}C analyses. Carbonate samples were analyzed at the MRL Key laboratory of Metallogeny and Mineral Assessment, Institute of Mineral Resources, Chinese Academy of Geological Sciences. A GasBench II continuous flow method was used with a

Table 1. Average monthly sea surface temperature and sea surface salinity during 2005 to 2009 on the northwest coast of Bohai Bay (Fan CF et al., 2012).

Month	JAN	FEB	MAR	APR	MAY	JUN	JUL	AUG	SEP	OCT	NOV	DEC
SSS/‰	31.6	31.5	31.7	31.5	31.4	31.3	29.8	29.5	30.2	30.6	30.6	31.2
SST/°C	−0.7	−0.5	3.4	10.3	16.9	21.9	25.4	27.1	24.0	18.3	10.4	3.0

MAT253 mass spectrometer. The systems consisted of a Thermo Finnigan GasBench II equipped with a CTC Combi-Pal autosampler linked to a MAT253 mass spectrometer. Carbonate micro-samples were manually loaded into 12 mL round-bottomed borosilicate exetainers and sealed using butyl rubber septa. Eighty-eight exetainers, including 18 aliquots of 4 China National Standards (GBW04405, GBW04406, GBW04416, and GBW04417), were routinely loaded in each sequence. The exetainers were automatically flushed with grade 5 He by penetrating the septa using a double-hole needle at a flow rate of 100 mL/min. Later, 4-6 drops of phosphoric acid were deposited in each exetainer. The exetainers were placed into an aluminum tray maintained at 72°C for 12 h. Subsequently, the sample gas was introduced 10 times into the mass spectrometer by sampling through the standard 100 μL sample loop, CO_2 is separated from other components using a gas chromatography column (Paroplot Q with fused-silica tubing, 25 mm×0.32 mm, Thermo Fisher Scientific) heated to 70°C. The peak corresponding to CO_2 was then passed through an open split into the mass spectrometer. The external precision of standards per run was typically 0.1‰ for $\delta^{13}C$ and $\delta^{18}O$.

4. Results

The authors analyzed 46, 42, and 77 consecutive samples from the modern shells ST2, ST25 and ST31, respectively. The $\delta^{18}O$ values of the measured samples showed a quasi-sinusoidal pattern (Figs. 3a, 4a and 5a). High $\delta^{18}O$ values imply lower temperatures (winters) and low values represent higher temperatures (summers) (Fan CF et al., 2011), hence, the highest oxygen isotope value in an annual cycle represents the interannual boundary, this helps recognize annual cycles in the $\delta^{18}O$ profiles. For the tested portions of the modern living shells ST2, ST25 and ST31, $\delta^{18}O$ values ranged between −3.25‰ to 1.85‰, −3.49‰ to 0.93‰, and −3.77‰ to 1.63‰, respectively (Table 2). From 2003 to 2004, based on the observations recorded from the three oyster shells, the average heaviest $\delta^{18}O$ value in winter was 1.47‰, the average lightest $\delta^{18}O$ value in summer was −3.50‰, and the average amplitude was 4.97‰ (Table 2). Their oxygen isotope curves were quasi-sinusoidal in shape, with negative peaks having wide half wavelengths, whereas the positive excursions were narrower. The spatial sampling resolution increased towards the younger increments because significantly more shell material was available (Ullmann C et al., 2010).

5. Discussion

5.1. Salinity- $\delta^{18}O_{water}$ relationship

Fan CF et al. (2011) reported that freshwater input into the northwest coast of the Bohai Bay is controlled mainly by the discharge of the Chaobai, Jiyunhe and Yongding rivers. Therefore, the authors, based on the measured salinities and oxygen isotope data (Fan CF et al., 2012) for the Chaobai, Jiyunhe and Yongding rivers, remove a discrete value and linear fitting to establish a "salinity-$\delta^{18}O_{water}$ model" (Fig. 6), which permitted the estimation of $\delta^{18}O_{water}$ directly from salinity measurements:

$$\delta^{18}O_{water,V\text{-}SMOW}‰ = 0.13 \times S - 4.89 (R = 0.99, N = 9), \quad (1)$$

where $\delta^{18}O_{water,\ V\text{-}SMOW}$ is the oxygen isotope composition of the water, S is the salinity in parts per thousand (‰), and subscript V-SMOM indicates that the volume fraction is based on SMOW (standard mean ocean water) in units of ‰, and converted from SMOW to the PDB scale described by Gonfiantini et al. (1995) as follows:

$$\delta^{18}O_{V\text{-}PDB} = (\delta^{18}O_{V\text{-}SMOW} - 30.91)/1.0309. \quad (2)$$

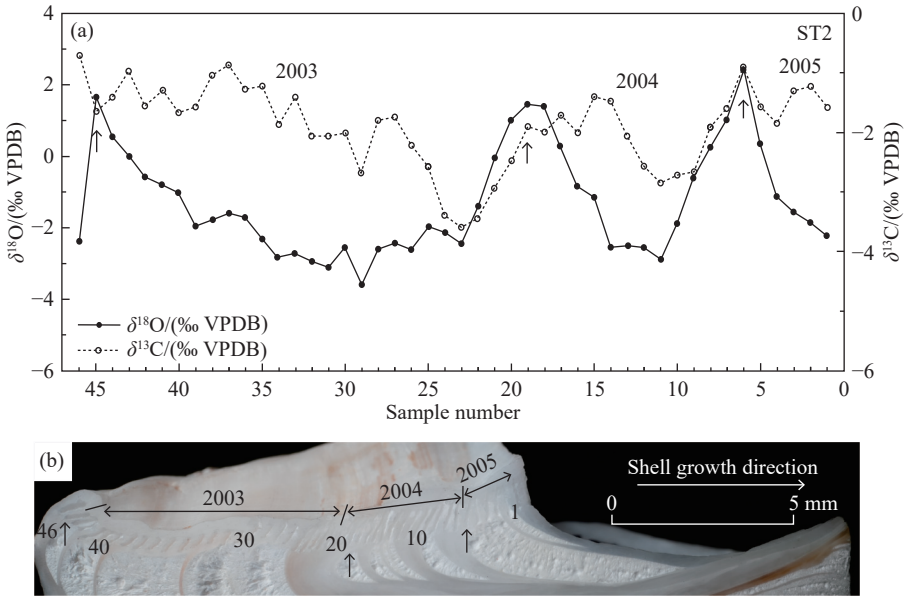

Fig. 3. Isotope values and morphology of the left valve of the modern living shell ST2. a– $\delta^{18}O$ and $\delta^{13}C$ profiles of a selected portion of shell within the ligament area. b–cross-sectional view of the ligament area in shell ST2, showing translucent growth bands and the locations of sample sites. Arrows show the locations of the growth layers that formed during low winter temperatures.

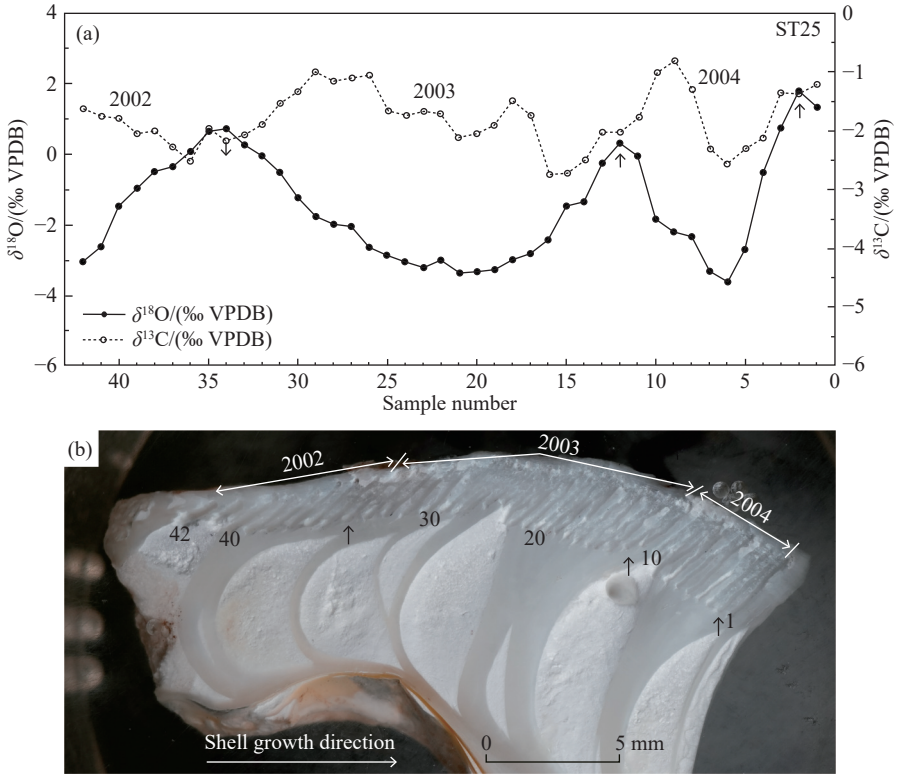

Fig. 4. Isotope values and morphology of the left valve of the modern living shell ST25. a–$\delta^{18}O$ and $\delta^{13}C$ profiles of a selected portion of shell within the ligament area. b–cross-sectional view of the ligament area in shell ST25, showing translucent growth bands and the locations of sample sites. Arrows are the same as in Fig. 3.

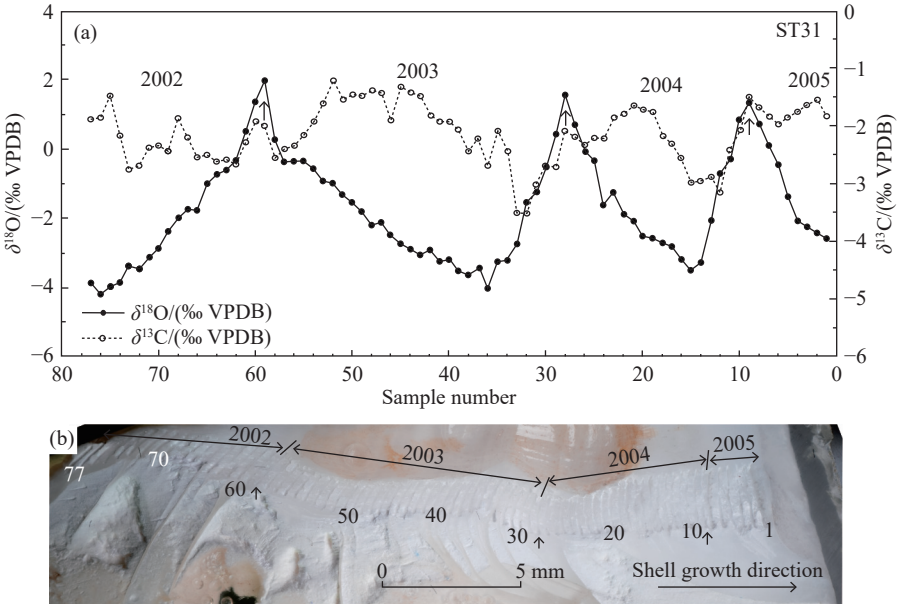

Fig. 5. Isotope values and morphology of the left valve of the modern living shell ST31. a–$\delta^{18}O$ and $\delta^{13}C$ profiles of a selected portion of shell within the ligament area. b–cross-sectional view of the ligament area in shell ST31, showing translucent growth bands and the locations of sample sites. Arrows are the same as in Fig. 3.

After the conversion of the SMOW standard to the PDB standard, the variation relationship between the water salinity and $\delta^{18}O$ in the Bohai Bay area can be expressed as follows:

$$\delta^{18}O_{water,V\text{-}PDB}‰ = 0.13 \times S - 34.73 \quad (3)$$

Consequently, 1‰ change in the northwest coast of Bohai Bay salinity equals a 0.13‰ change in seawater $\delta^{18}O_{V\text{-}PDB}$.

5.2. *C. gigas* winter freeze shock temperature

Oxygen isotope fluctuations in calcite shells are mainly reflection of ambient seawater temperatures and salinity

Table 2. Lightest and heaviest $\delta^{18}O$ values among consecutive micro-growth layers of shells, and corresponding fluctuation.

Specimens	Minimum /VPDB‰	Mean	Maximum /VPDB‰	Mean	Fluctuation /‰
ST2	−2.89	−3.25	2.44	1.85	5.10
	−3.61		1.44		
			1.66		
ST25	−3.61	−3.49	1.75	0.93	4.42
	−3.37		0.31		
			0.72		
ST31	−3.51	−3.77	1.34	1.63	5.40
	−4.03		1.56		
			1.98		
ST2, ST25, ST31		−3.50		1.47	4.97

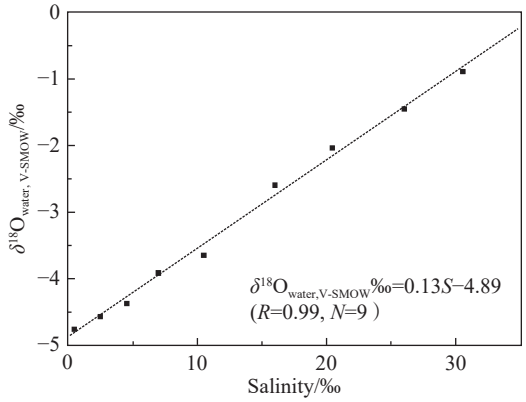

Fig. 6. Salinity-$\delta^{18}O_{water}$ relationship of the estuaries water in the living oyster reef area of Bohai Bay (modified from Fan CF et al., 2012).

(Epstein S et al., 1953; Tarutani T et al., 1969; Kirby MX et al., 1998). The observed $\delta^{18}O$ cyclicity in the *C. gigas* shell (Figs. 3a, 4a, and 5a) is a reflection of annual temperature and salinity fluctuations in sea surface water along the northwest coast of the Bohai Bay. Based on the temperature dependent fractionation of oxygen (−0.24 to −0.25‰/°C, Epstein S et al., 1953), the $\delta^{18}O$ amplitudes of all the shells can be attributed to water temperature changes. The $\delta^{18}O$ average amplitude of the three samples was 4.97‰, which would require temperature variations of approximately 20.3°C (19.9°C–20.7°C) if water temperatures were the only cause of the $\delta^{18}O$ fluctuation in the shell. However, seasonal changes in seawater $\delta^{18}O$ of these living oyster shells must also be taken into consideration (Ullmann C et al., 2010).

The oyster shell $\delta^{18}O$ was influenced by temperature and salinity in opposing ways (Ullmann C et al., 2010; Fan CF et al., 2012). Seawater $\delta^{18}O$ depends on the degree of freshwater influx and precipitation, often resulting in a positive correlation between salinity and seawater $\delta^{18}O$ (Fig. 2). Warmer waters in the summer months produce lower $\delta^{18}O$, while the seawater is simultaneously enriched with ^{16}O due to increased riverine influx and precipitation. On the other hand, cooler waters in the winter months produce higher $\delta^{18}O$, while the seawater is simultaneously enriched with ^{18}O due to decreased riverine influx and precipitation. Therefore, the calculated temperature fluctuations are over estimates that do not take into account the reductions caused by changes in seawater $\delta^{18}O$ or salinity, and the real temperature variation must have been in less than 20.3°C.ature variation must have been in less than 20.3°C.

The SST records in the study area indicated that the highest present-day water temperature was 27.5°C, in addition, oyster shells in the study area showed no evidence that they had experienced summer heat shocks among growth bands viewed in the cross sections (Figs. 3a, 4a, and 5a, Fan CF et al., 2010; Fan CF et al., 2011). These observations implied that the oyster shell recorded the highest seawater temperature in this area, and the lightest shell $\delta^{18}O$ value corresponded to the highest water temperature and the lowest water salinity in summer. Therefore, discrepancies between the $\delta^{18}O$ amplitude recorded by living oyster shells and the seasonal variation amplitude of its growing environment, were contributions of low water temperature and high salinity in winter, and had no correlations with high water temperature and low salinity in summer(Ullmann C et al., 2010).

From winter to summer, the water salinity in the shell growth area varies from 31.7‰ to 29.5‰ (Fan CF et al., 2012), with a variation range of 2.2‰. However, as oyster stop secreting shell during winter, the maximum annual salinity variations cannot be used for calculations simply.

The results calculated without considering the salinity effect showed that the shells resumed growth from March end to the beginning of April (>7.2°C) (Fan CF et al., 2012), but the environment information for March was not fully recorded in the shell due to the winter freeze shock. Therefore, the average salinity from March to April (31.6‰) was used for calculating. The oyster shells recorded a salinity range of 29.5–31.6‰, and its contribution to the changes in water $\delta^{18}O$ was 0.27‰ VPDB. Considering this contribution to water $\delta^{18}O$, the average water temperature variation range recorded by ST2, ST25, and ST31 shells was 19.2°C (18.8°C–19.6°C).

Therefore, it can be calculated that the oysters stopped or retarded secreting their shells, and living environment information on the micro-growth layers was not fully recorded when the water temperature was below 8.3°C in winter.

According to the $\delta^{18}O$ records of modern oyster shells in the Bohai Bay area and the hydrological data of live oysters in growing waters, oyster shell calcification stopped or retarded in winter, at water temperatures below 8.3°C. This water temperature was lower than the minimum water temperature at which shell secretion ceases at 11.5°C(Wang H et al., 1995), which was calculated by Epstein S et al.'s equation (1953) that data from $\delta^{18}O$ values recorded for modern living shell in Xiaoqinghe River estuary (Shandong, China) and Yerseke estuary of the Oosterscheld River (Zeeland, Netherlands). Ullmann C et al. (2010) used the measured monthly resolution oxygen isotope recordings from a live oyster (*C. gigas*) shell grown in the North Sea to calculate that the water temperature at which shell secretion stops is about 6°C.

These three modern living specimens of *C. gigas* (ST2, ST25, and ST31) were collected on May 26, 2005, from a living oyster reef, where local oysters had spawned and resumed growth (Fan CF et al., 2011; Fan CF et al., 2012). According to the monthly average water temperature data of the Bohai Bay area, if the minimum water temperature at which *C. gigas* halted or retarded shell secretion in winter was 11.5°C, the oysters would resume normal growth in April (Table 1), with a time interval of only 1–2 months, from April until the specimen collection time. However, during this period, oysters resumed normal growth and also experienced slow growth in the spawning season (Fan CF et al., 2011; Fan CF et al., 2012). According to the above mentioned actual circumstance, the water temperature for growth resumption in *C. gigas* should be lower than 11.5°C and the time for growth resumption should be earlier. This study showed that the live oysters in the Bohai Bay area resumed growth at the end of March when the average water temperature was approximately 8°C. Therefore, 8.3°C was adopted as the minimum water temperature for *C. gigas* to halt shell secretion during winter in the Bohai Bay area.

Shell $\delta^{18}O$ may not reflect the complete annual seawater temperature variation, particularly at middle and high latitudes, and can be devoid of the lowest water temperature signal. For example, the maximum $\delta^{18}O$ values in an annual growth cycle of oyster shells recorded the growth information during December and March of the following year, and shell secretion was discontinuous when the water temperature was below 8.3°C. However, beside the water temperature, there are many other factors that affect the growth of shells, such as salinity, sediment deposit rate, food source and even difference between individuals, etc. Therefore, on average while the water temperate decrease to 8.3°C the shell secretion will cease.

5.3. Implication for C. gigas' carbon sink potential

Oysters fix carbon directly in two ways. One is to convert HCO_3^- in water into $CaCO_3$ shells by calcification, thereby fixing a large amount of carbon. Another is to promote the growth of individual soft tissues by filtering particulate organic carbon (POC) in seawater, a process called biosynthesis. In addition, biodeposition by oysters can transport large volumes of organic carbon in the form of faeces and pseudofaeces to the oyster reef sediment, thus indirectly playing the role of biological carbon sink (Fodrie FJ et al., 2017). Calcification is considered to be the main ecological process of carbon sequestration in oysters (Shen XQ et al., 2011; Li J et al.,2016; Zhang YY et al., 2017), the annual carbon sequestration per unit area produced by calcification in oyster reef area is about 2.7kg/m^2 (Shen XQ et al., 2011).

The calcification of oysters slowed down or stopped during winter freeze shock, and the biosynthesis and biodeposition were also affected by oyster freeze shock. In this study, the freeze shock temperature of the shell calculated by the modern oyster shell is 8.3°C, which is lower than the freeze shock temperature (11.5°C) calculated by Wang H et al. (1995) using the modern living oyster shells. The decrease of the winter freezing shock temperature means the extension of the shell growth time in one year. If the shell stop or retard secreting at 11.5°C, it means the shell growth time is from mid-April to mid-November. While the shell stop or retard secreting decrease to 8.3°C, the shell growth will start at end of March and stop at end of November. Therefore, the calcification time of oysters within one year is nearly a month longer than previously thought. Influenced by global warming, global sea surface temperature trend to be warming. A suitable sea surface temperature environment can promote the rapid and healthy growth of oyster shells, increase their carbon sequestration time and improve carbon sink potential (Shen XQ et al., 2011; Wang H et al., 1995).

6. Conclusions

The water temperature that suffer from winter freeze shock and stops or retards the growth of Pacific oysters in Bohai Bay is about 8.3°C, and the normal growing season for oysters in this area was from end of March to end of November. The maximum $\delta^{18}O$ values in an annual growth cycle of oyster shells recorded the growth environment information when the shells stopped secreting in December and when the shells resumed growth in March of the following year. As the water temperature was below about 8.3°C (between December and March), the oysters stopped or retarded secreting shells, and the growth environment information could not be fully recorded.

The winter freeze shock temperature of the shell calculated by the modern oyster shells in northwest of Bohai Bay are lower than previously estimated. The calcification time of oysters within one year is nearly a month longer than previously thought, therefore, its carbon sink potential is also improved.

CRediT authorship contribution statement

Wen-yu Wang and Chang-fu Fan developed the theoretical formalism and performed the analytic calculations. Wen-yu Wang wrote the manuscript with support from Chang-fu Fan. All authors discussed the results and contributed to the final manuscript.

Declaration of competing interest

The authors declare no conflicts of interest.

Acknowledgments

The authors thank Professors Yi Liu, Ya-ping Wang, and Jian-fen Li for their valuable suggestions on the revision of this article. Thanks to Yan-dong Pei, Li-zhu Tian, and Zhi-wen Shang for assisting with sample collection and environmental monitoring. This research received financial support from NSFC (Account 41473013, 40872106, and 41627802).

References

Arrhenius S. 1896. On the influence of carbonic acid in the air upon the temperature on the ground. The Philosophical Magazine, 41(251), 237–276. doi: 10.1080/14786449608620846.

Broecker WS, Takahashi T. 1996. Calcium carbonate precipitation on the Bahama banks. Journal of Geophysical Research, 71(6), 1575–1602. doi: 10.1029/JZ071i006p01575.

Cognie B, Haure J, Barille L. 2006. Spatial distribution in a temperate coastal ecosystem of the wild stock of the farmed oyster *Crassostrea gigas* (Thunberg). Aquaculture, 259(1−4), 249–259. doi: 10.1016/j.aquaculture.2006.05.037.

Diederich S. 2005. Differential recruitment of introduced Pacific oysters and native mussels at the North Sea coast: coexistence possible? Journal of Sea Research, 53(4), 269−281. doi: 10.1016/j.seares.2005.01.002.

Dame RF. 1987. The net flux of inorganic matter by an intertidal oyster reef. Continental Shelf Research, 7(11–12), 1421–1424. doi: 10.1016/0278-4343(87)90048-3.

Dame RF, Spurrier JD, Wolaver TG. 1989. Carbon, nitrogen and phosphorusprocessing by an oyster reef. Marine Ecology Progress Series, 54(3), 249–256.

Epstein S, Buchsbaum R, Lowenstam H, UREY HC. 1953. Revised carbonate-water isotopic temperature scale. Geo Science World, 64(11), 417–426. doi: 10.1130/0016-7606(1953)64[1315:RCITS]2.0.CO;2.

Fan CF, Pei YD, Wang H, Koeniger P, Li YH. 2010. Stable isotope sclerochronology study of oyster shells. Advances In Earth Science, 25(02), 163–173 (in Chinese with English abstract). doi: 10.11867/j.issn.1001-8166.2010.02.0163.

Fan CF, Wang H, Pei YD, Wang HF. 2012. The lowest sea surface temperatures for stopping secretion in winter and resuming growth in spring recorded by the living Pacific oyster (*Crassostrea gigas*) shell in the Bohai Bay. Acta Geoscientica Sinica, 33(06), 953–960 (in Chinese with English abstract). doi: 10.1007/s11783-011-0280-z.

Fan CF, Koeniger P, Wang H, Frechen M. 2011. Ligamental increments of the mid-Holocene Pacific oyster *Crassostrea gigas* are reliable independent proxies for seasonality in the western Bohai Sea, China. Paleogeography, Paleoclimatology, Paleoecology, 299(3–4), 437–448. doi: 10.1016/j.palaeo.2010.11.022.

Fodrie FJ, Rodriguez AB, Gittman RK, Grabowski JH, Lindquist NL, Peterson CH, Piehler MF, Ridge JT. 2017. Oyster reefs as carbon sources and sinks. Proceedings of The Royal Society B: Biological Sciences, 284, 20170891. doi: 10.1098/rspb.2017.0891.

Gonfiantini R, Stichler W, Rozanski K. 1995. Standards and intercomparison materials distributed by the International Atomic Energy Agency for stable isotope measurements. Reference & Intercomparison Materials For Stable Isotopes of Light Elements, 27, 13–29.

Gao LJ, Shen AL, CHEN YQ, Han JD. 2006. Determination of filtration rate of *Crassostrea sp*. Marine Environmental Science, 25(4), 62–65 (in Chinese with English abstract). doi: 10.3969/j.issn.1007-6336.2006.04.017.

Hainbucher D, Hao W, Pohlmann T, Sündermann J, Feng SZ. 2004. Variability of the Bohai Sea circulation based on model calculations. Journal of Marine Systems, 44(3/4), 153–174. doi: 10.1016/j.jmarsys.2003.09.008.

Jackson JB, Kirby MX, Berger WH, Bjorndal KA, Botsford LW, Bourque BJ, Bradbury RH, Cooke R, Erlandson J, Estes JA, Hughes TP, Kidwell S, Lange CB, Lenihan HS, Pandolfi JM, Peterson CH, Steneck RS, Tegner MJ, Warner RR. 2001. Historical over-fishing and the recent collapse of coastal ecosystems. Science, 293(5530), 629–637. doi: 10.1126/science.1059199.

Li JF, Shang ZW, Chen YS Tian LZ, Jiang YX, Wang F, Hu YZ, Wang F, Yang P, Wen MZ, Yuan HF, Shi PX, Wang H. 2020. Research status and protection suggestions on oyster reef in Bohai Bay. Geological Survey And Research, 43(04), 317–333 (in Chinese with English abstract). doi: 10.3969/j.issn.1672-4135.2020.04.003.

Li J, Gong PH, Guan CT, Liu Y. 2016. Carbon sequestration of additives of artificial reefs and its effect on carbon fixation of Ostrea plicatula Gmelin. Progress In Fishery Sciences, 37(6), 100–104 (in Chinese with English abstract). doi: 10.11758/yykxjz.20151215002.

Kirby MX, Soniat TM, Spero HJ. 1998. Stable isotope sclerochronology of pleistocene and recent oyster shells (*Crassostrea virginica*) . PALAIOS, 13(6), 560–569. doi: https://doi.org/10.2307/3515347.

Peterson CH, Grabowski JH, Powers SP. 2003. Estimated enhancement of fish production resulting from restoring oyster reef habitat: Quantitative valuation. Marine Ecology Progress Series, 264(Dec), 249–264.doi. doi: 10.1007/s12665-015-5056-5.

Peterson CH, Lipcius RN. 2003. Conceptual progress towards predicting quantitative ecosystem benefits of ecological restorations. Marine Ecology Progress Series, 264(Dec), 297–307. doi: 10.3354/meps264297.

Quan WM, Shen X, Luo M, Chen Y. 2006. Ecological function and restoration measures of oyster reef in estuaries. Chinese Journal of Ecology, 25(10), 1234–1239 (in Chinese with English abstract). doi: 10.1016/S1872-2032(06)60052-8.

Quan WM, Zhan JP, Ping XY, Shi LY, Li PJ, Chen YZ. 2007. Purification function and ecological service value of *Crassostrea sp*. in Yangtze River estuary. Chinese Journal of Applied Ecology, 18(4), 871–876 (in Chinese with English abstract).

Shen XQ, Quan WM, Yuan Q. 2011. Restoration and assessment of carbon sink potential for an intertidal oyster reef in the Yangtze River Estuary, China. Journal of Agro-Environment Science, 30(10), 2119–2123 (in Chinese with English abstract). doi: 10.1080/00405000.2010.522047.

Tarutani T, Clayton RN, Mayeda TK. 1969. The effect of polymorphism and magnesium substitution on oxygen isotope fractionation between calcium carbonate and water. Geochimica et Cosmochimica Acta, 33(8), 987–996. doi: 10.1016/0016-7037(69)90108-2.

Taylor AH, Watson AJ, Ainsworth M, Robertson JE, Turnere DR. 1991. A modelling investigation of the role of phytoplankton in the balance of carbon at the surface of the North Atlantic. Global Biogeochem Cycles, 5(2), 151–171. doi: 10.1029/91GB00305.

Ullmann C, Wiechert U, Korte WC. 2010. Oxygen isotope fluctuations in a modern North Sea oyster (*Crassostrea gigas*) compared with annual variations in seawater temperature: Implications for paleoclimate studies. Chemical Geology, 277(1–2), 160–166. doi: 10.1016/j.chemgeo.2010.07.019.

Wang H, Keppens E, Nielsen P, Riet AV. 1995. Oxygen and carbon isotope study of the Holocene oyster reefs and paleoenvironmental reconstruction on the northwest coast of Bohai Bay, China. Marine Geology, 124(1–4), 289–302. doi: 10.1016/0025-3227(95)00046-2.

Wang H, Fan CF, Li JF, Li FL, Yan YZ, Wang YS, Zhang JQ, Zhang YF. 2006. Holocene oyster reefs on the northwest coast of the Bohai Bay, China. Geological Bulletin of China, 25(03), 315–331 (in Chinese with English abstract).

Yang P, Li JF, Wang F, Hu YZ, Shi BJ, Wang WY, Wang H. 2022. Present situation and protection restoration suggestions on the natural oyster reefs in China. Geology in China, 50(4), 1082–1092 .

Zou HL. 1988. A preliminary exploration of climatic change in the Bohai region in recent hundred years. Marine Forecasts, (4), 14–19 (in Chinese with English abstract).

Zhang YY, Zhang JH, Ling YT, Li HM, Li G, Chen X, Zhao P, Jiang ZJ, Zou DH, Liu XY, Liu JH. 2017. Formation process and mechanism of carbon sink in China's offshore aquaculture environment. Scientia Sinica Terrae, 47(12), 1414–1424 (in Chinese with English abstract). doi: 10.1360/N072017-00344.